Canadian Mineralogist
Vol. 17, pp. 719-728 (1979)

THE CHEMICAL COMPOSITION AND INFRARED SPECTRUM OF NICKEL- AND IRON-SUBSTITUTED SERPENTINE FROM A NICKELIFEROUS LATERITE PROFILE, SOROAKO, INDONESIA

J. PAUL GOLIGHTLY
INCO Metals Company, Sheridan Park, Mississauga, Ontario L5K 1Z9

OLGA N. ARANCIBIA
Dept. of Geological Sciences, Queen's University, Kingston, Ontario K7L 3N6

ABSTRACT

Nickel- and iron-substituted lizardites from a nickeliferous laterite ore profile at Soroako, Indonesia, have been studied. Microprobe data show that orthopyroxenes have lost 50% of their Al content to neighboring olivine pseudomorphs during serpentinization. However, Ni, Mg, Cr and Fe contents of lizardite pseudomorphs after olivine and orthopyroxene are identical to those of their host minerals. Weathered lizardites have a reduced Mg content and increased Fe, Al, Cr and Ni contents relative to unweathered lizardites. There is a strong correlation of nickel and iron values, and no significant difference in the Ni and Fe content of weathered olivine and orthopyroxene pseudomorphs. A silica excess in the calculated formulae suggests that these minerals may be intermediate between nickeliferous lizardite and a dioctahedral ferric analogue of kaolinite. The relative infrared intensity of the OH libration band at 610 cm^{-1} is proportional to the magnesium occupancy of trioctahedral sites. This indicates a highly inhomogeneous or ordered substitution by Ni or Fe.

SOMMAIRE

Nous avons examiné les lizardites nickelifères et ferrifères du gisement de latérite nickelifère de Soroako (Indonésie). Les analyses à la microsonde montrent que, durant la serpentinisation, les orthopyroxènes ont cédé à des pseudomorphes d'olivine avoisinants la moitié de leur Al. Par contre, les teneurs en Ni, Mg, Cr et Fe de la lizardite qui remplace l'olivine et l'orthopyroxène sont identiques à celles des minéraux originels. Les lizardites altérées ont perdu du Mg et se sont enrichies en Fe, Al, Cr et Ni par rapport aux lizardites saines. Fe et Ni sont fortement en corrélation, avec teneurs presque identiques dans les pseudomorphes de l'olivine et de l'orthopyroxène. Vu l'excédent de silice dans les formules calculées, ces minéraux pourraient être des termes intermédiaires entre la lizardite nickelifère et l'analogue ferrique dioctaédrique de la kaolinite. Dans l'infrarouge, l'intensité relative de la bande de libration OH à 610 cm^{-1} est proportionnelle à la population de Mg des sites trioctaédriques, ce qui caractériserait la substitution du Ni ou du Fe comme très hétérogène ou ordonnée.

(Traduit par la Rédaction)

INTRODUCTION

Relatively little has been published on the properties and paragenesis of nickeliferous serpentines. Existing data usually refer to highly nickeliferous specimens, generally from museum collections, with little reference to the mode of origin of the mineral. The present paper fills this gap to some degree with specimens that show intermediate levels of nickel substitution, and also provides infrared-absorption data for nickeliferous lizardite. These data shed some light on absorption-band assignments in serpentines. The specimens are typical of nickeliferous serpentine in laterite ore deposits, a major source of nickel.

OCCURRENCE

The specimens investigated come from a deep lateritic weathering profile overlying serpentinite and serpentinized lherzolite in the vicinity of the P.T. International Nickel mine at Soroako, on the island of Sulawesi (formerly Celebes), Indonesia. The weathering profile is about 18 m thick and is located on a saddle ridge between two hills standing about 20 m above a ferricrete-covered plateau. The upper 9 m consist of a fine-grained goethite laterite containing minor amounts of talc and chromian spinel inherited from the parent rock. Below this level is an irregular, intertonguing saprolitic transition zone between the goethite laterite and the serpentinized lherzolite parent rock. The nickeliferous serpentines examined were obtained from boulders in the lower portion of the profile, in the zone of saprolitized peridotite. Weathered serpentine in samples of saprolite from the 9–12 m depth interval were analyzed by Arancibia (1975) by electron microprobe, and infrared analyses were done by Golightly on material from the same depth interval. Microprobe analyses of unweathered serpentine from a saprolite boulder were done at INCO by M. Sizgoric.

Additional general information on the local and regional geology is given by Golightly (1979b), Soeria-Atmadja *et al.* (1974) and P.T. International Nickel (1972). A detailed mineralogical and chemical study of the particular profile is reported by Arancibia (1975).

PETROGRAPHY

The bedrock varies in composition from lherzolite to dunite. For the most part, the olivines have been altered to mesh-textured lizardite, and the orthopyroxenes have been replaced by "bastite" lizardite pseudomorphs. The saprolite shows all the primary textural features of serpentine in fine detail, so that there is no doubt that the changes in chemical composition indicated by the microprobe analyses are the result of pseudomorphism reactions. The optical orientation of the lizardite is unaffected by weathering, suggesting that the silicate structures have not been seriously disrupted. The saprolites consist largely of yellow to yellow-orange nickeliferous serpentine with minor amounts of fine-grained goethite distributed in zones within the mesh texture in positions normally occupied by zones of magnetite grains in the unweathered serpentine.

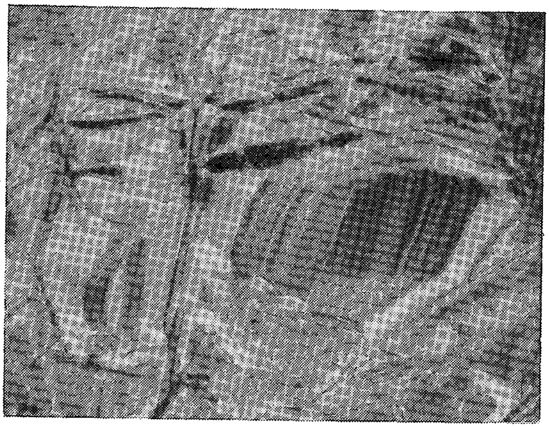

FIG. 1. The photograph shows two cells of mesh-textured serpentine pseudomorphic after olivine. The dark-banded "eyes" consist of unweathered lizardite containing abundant black magnetite grains. In the lighter grey, outermost zones of the eyes and in the smaller, upper right-hand "eye", the light core consists of weathered lizardite.

TABLE 1. SOROAKO, MICROPROBE ANALYSES* OF UNWEATHERED SERPENTINES

	AFTER OLIVINE	"BASTITE" AFTER ORTHOPYROXENE
NiO	0.28	0.05
FeO	5.76	8.31
Al_2O_3	†	1.53
Cr_2O_3	-	0.83
MgO	38.3	36.2
SiO_2	39.3	36.2
TOTAL	83.6	83.1
	STRUCTURAL FORMULAE	
Si	1.955	1.851
Al	.000	.092
Cr	.000	.034
Fe^{3+}	.045	.023
Σtet	2.000	2.000
Mg	2.832	2.750
Fe	.195	.331
Ni	.012	.002
Σoct	3.035	3.083

Analyses are composites of about six points. Replicate analyses on the same points for all analyses were impossible due to specimen sputtering.

†Significant Al signals indicating up to 0.6 Al_2O_3 were noted at about half individual locations but the peak to background ratio was not sufficient to support an average Al_2O_3 figure.

*Weight percent.

The boundary between weathered and unweathered serpentine is occasionally visible in thin section (Fig. 1) in the vicinity of 1–2 cm "eyes" of relatively unserpentinized lherzolite. At this boundary, the heterogeneous intergrowth of mesh lizardite with magnetite changes abruptly to an optically homogeneous yellow to yellow-orange serpentine without magnetite but with the same optical orientation as the primary lizardite. It seems that most of the submicron-scale magnetite grains have been abruptly resorbed into the serpentine at this boundary with a minor amount of the coarser magnetite being replaced by goethite.

Powder X-ray-diffraction patterns of several grains of bastite and mesh-textured serpentine compare well with the pattern of lizardite (Whittaker & Zussman 1956). However, the possibility that minor chrysotile is present as veinlets in some of the material cannot be ruled out. The samples contain accessory amounts of chromian spinel and, where unweathered, traces of pentlandite and chalcopyrite.

CHEMICAL COMPOSITION OF SERPENTINE

Microprobe analyses of unweathered lizardite grains derived from olivine and orthopyroxene are given in Table 1. Analyses of weathered specimens are given in Tables 2, 3 and 4.

Weathered lizardites were analyzed at Queen's University by Arancibia (1975), using an Applied Research Laboratories electron microprobe (model AMX). All elements except nickel were determined using energy-dispersive analysis and compared to a series of pure reference spectra using a least-squares program. Nickel was determined by wavelength-dispersive analysis using nickel metal as standard. The excitation potential was 15 kV; a slightly defocused beam was used to minimize sputtering.

The unweathered lizardites were analyzed at INCO Metals Ltd., J. Roy Gordon Research Lab. at Mississauga by M.B. Sizgoric using an Acton–CAMECA model MS64 electron microprobe. All elements were determined by wavelength-dispersive analysis using an olivine standard for nickel, iron, magnesium and silicon and a hornblende standard for aluminum and chromium.

Fine magnetite and goethite inclusions in the lizardites were carefully avoided when selecting points for analysis. Evidence that the exclusion of particulate impurities was successful is presented below under nickel- and iron-substitution chemistry.

The oxide totals of the analyses are generally below the ideal. This could reflect extra water either held in micropores or present in addition to stoichiometric hydroxyl water, or both. Bulk chemical analyses (done at INCO) suggest that virtually all the iron in the weathered serpentines is ferric.

The structural formulae of the weathered lizardites show a marked deficiency in octahedral cations that increases with increasing Ni and Fe substitution. However, the Fe is ferric and the formulae as written give the positive charge required to balance the negative charge of 14. The crystal chemistry could be understood as being made up of three components with Mg in a trioctahedral lizardite structure, Ni in a trioctahedral nepouite structure and Fe in a dioctahedral ferric analogue of the kaolinite structure. The serpentine is, therefore, intermediate between a fully trioctahedral and a fully dioctahedral structure. Certain of the iron-rich serpentines from the Stillwater complex, analyzed by Wicks & Plant (1979) also give a large excess of silica. These have a petrographic appearance very similar to the weathered serpentines studied here. Brindley & Wan (1975) found a similar excess of silica. They, however, recalculated their chemical analyses of Ni-substituted lizardites and nepouites to give a trioctahedral formula. Brindley (1978) has observed occasional 9 Å layers in nickeliferous lizardites but has hesitated to explain all of the silica excess this way, preferring to attribute much of it to leaching of octahedral material at crystal-plate edges in extremely fine-grained specimens.

That the silica excess reflects occasional layers that have been converted to either a talc or a smectite structure with a net removal of divalent cation is difficult to apply to the Soroako situation. A direct replacement of serpentine by smectite minerals occurs in some nickeliferous laterite profiles (Golightly 1979a) but does not seem to have occurred at Soroako. There is no evidence of this type of structure either in the X-ray-diffraction patterns or in infrared-absorption spectra. If the silica excess in these samples were due to the incipient stages of such an alteration, more complete

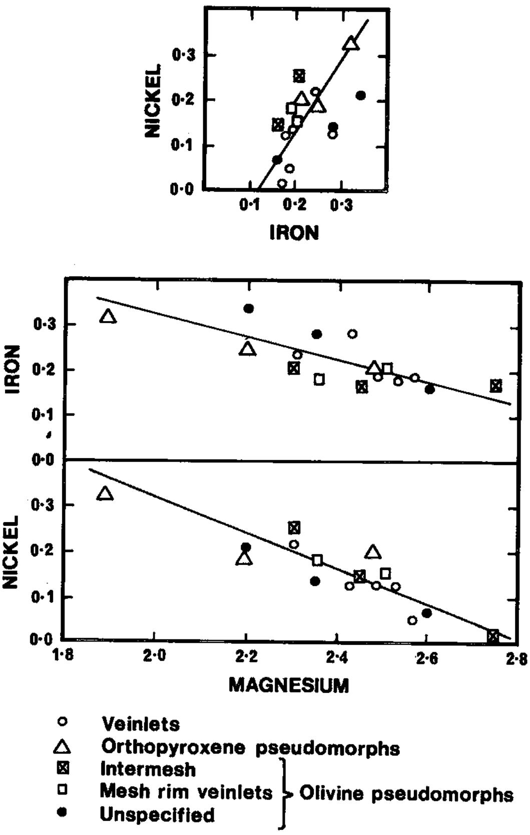

FIG. 2. Systematic correlations of nickel, iron and magnesium formula weights in nickel–iron substituted lizardites from Soroako.

reaction products would be expected in more evolved specimens. Smectite minerals, however, are nowhere present in this profile. Only traces of talc, inadequate to explain the silica excess in the lizardite, are observed in the goethite zone of the profile.

TABLE 2. MICROPROBE ANALYSES* OF WEATHERED SERPENTINE OLIVINE PSEUDOMORPHS

NiO	0.43	3.60	6.39	3.88	4.42
K_2O	0.00	0.00	0.09	0.04	0.00
Na_2O_3	0.00	0.00	0.00	0.00	0.00
CaO	0.06	0.04	0.11	0.03	0.08
MnO	0.10	0.12	0.01	0.24	0.18
MgO	37.95	33.94	31.28	33.86	30.42
Cr_2O_3	0.07	0.00	0.20	0.00	0.01
TiO_2	0.05	0.02	0.00	0.03	0.13
Fe_2O_3	6.15	4.40	5.55	5.39	4.95
Al_2O_3	0.71	0.39	0.83	0.46	0.48
SiO_2	39.13	41.16	40.85	39.99	39.30
TOTAL	84.65	83.67	85.31	83.92	79.97
			STRUCTURAL FORMULAE		
Si	1.906	2.034	2.019	1.989	2.047
Al	0.041	-	-	0.011	-
Fe^{+3}	0.053	-	-	-	-
Σ_{tet}	2.00	2.034	2.019	2.00	2.047
Al	0.0	0.023	0.048	0.016	0.029
Fe^{3+}	0.172	0.164	0.206	0.202	0.194
Ti	0.022	0.001	-	0.001	0.005
Cr	0.003	-	0.008	-	-
Mg	2.756	2.449	2.305	2.510	2.362
Mn	0.004	0.006	-	0.010	0.008
Ca	0.003	0.002	0.006	0.002	0.004
Na	-	-	-	-	-
K	-	-	0.006	0.003	-
Ni	0.017	0.145	0.254	0.155	0.185
Σ_{oct}	2.957	2.839	2.833	2.699	2.787

*Weight Percent

TABLE 3. MICROPROBE ANALYSES* OF WEATHERED SERPENTINE ORTHOPYROXENE PSEUDOMORPHS

NiO	5.03	4.64	7.49
K_2O	0.05	0.03	0.00
Na_2O_3	0.00	0.00	0.00
CaO	0.03	0.04	0.00
MnO	0.17	0.15	0.00
MgO	33.35	28.81	23.14
Cr_2O_3	0.63	0.81	0.66
TiO_2	0.00	0.04	0.00
Fe_2O_3	5.97	6.56	7.72
Al_2O_3	1.38	1.90	1.53
SiO_2	38.23	39.09	37.48
TOTAL	82.06	84.84	78.02
		STRUCTURAL FORMULAE	
Si	1.907	2.000	2.055
Al	0.081	-	-
Fe^{+3}	0.012	-	-
Σtet	2.00	2.00	2.055
Al	-	0.115	0.099
Fe^{3+}	0.212	0.253	0.319
Ti	-	0.002	-
Cr	0.025	0.033	0.029
Mg	2.479	2.197	1.891
Mn	0.007	0.006	-
Ca	0.002	0.002	-
Na	-	-	-
K	0.003	0.002	-
Ni	0.202	0.191	0.330
Σoct	2.930	2.801	2.668

*Weight Percent

TABLE 4. MICROPROBE ANALYSES* OF WEATHERED SERPENTINE VEINLETS OF UNCERTAIN PARENTAGE

NiO	1.32	3.14	3.19	3.21	5.41
K_2O_3	0.02	0.04	0.00	0.00	0.01
Na_2O	0.00	0.00	0.00	0.00	0.01
CaO	0.05	0.00	0.09	0.05	0.08
MnO	0.00	0.00	0.17	0.10	0.18
MgO	35.11	34.67	33.82	33.47	30.83
Cr_2O_3	0.01	0.24	0.02	0.06	0.00
TiO_2	0.00	0.06	0.06	0.03	0.01
Fe_2O_3	5.17	4.92	5.25	7.75	6.38
Al_2O_3	0.16	0.36	0.65	0.85	0.68
SiO_2	41.41	40.97	40.78	40.23	40.27
TOTAL	83.25	84.40	84.03	85.97	83.86
			STRUCTURAL FORMULAE		
Si	2.035	2.009	2.011	1.969	2.019
Al	-	-			
Fe^{+3}	-	-	-	-	-
Σ_{tet}	2.035	2.009	2.011	2.00	2.019
Al	0.009	0.021	0.038	0.018	0.040
Fe^{3+}	0.191	0.182	0.195	0.283	0.241
Ti	-	0.002	0.002	0.001	-
Cr	-	0.009	0.001	0.002	-
Mg	2.572	2.534	2.486	2.427	2.306
Mn	-	-	0.007	0.004	0.008
Ca	0.003	-	0.005	0.003	0.004
Na	-	-	-	-	0.005
K	0.001	0.002	-	-	0.001
Ni	0.052	0.124	0.127	0.126	0.218
Σ_{oct}	2.828	2.874	2.861	2.864	2.823

* Weight Percent

Supporting evidence of a negative nature comes from the analyses, both chemical and microprobe, of "serpentine–garnierites" from a number of Brazilian localities by Esson & Carlos (1978). These workers found no silica excess, but their specimens contain far less iron than the Soroako ones.

The bulk of evidence from Soroako tends to support the idea that the silica excess is largely associated with the substitution of ferric iron in the serpentine structure and that the structure is intermediate between a trioctahedral nickeloan lizardite and a dioctahedral ferric analogue of kaolinite.

Microprobe analyses of unaltered serpentine in Table 1 show the opposite tendency, a slight excess in the octahedral position. Possibly, there is intergrown submicroscopic brucite in the fresh material, as found by Page (1967) and Wicks & Whittaker (1977). Brucite was not detected, however, by XRD (114.6 mm-radius powder camera) in material dug out of the probe site. Submicron-range magnetite particles inadvertently included could also contribute to, but not completely explain, the apparent excess in the octahedral position.

SUBSTITUTION CHEMISTRY

Nickel and iron

The nickel grades of the unweathered serpentines clearly reflect those of the parent minerals. The mesh-textured lizardites have nickel values (0.21%) only slightly lower than those of olivine (0.34%), and the bastites have a very low nickel level (~0.040%), comparable to the levels in orthopyroxene (0.063%: Arancibia 1975).

The iron/magnesium atomic ratio in bastite lizardite (0.1287) is significantly higher than that in the mesh-textured lizardite (0.0845), whereas the ratios in orthopyroxene (0.0987) and olivine (0.108) are about equal. This is undoubtedly due in part to the widespread crystallization of magnetite throughout the mesh-textured lizardite, leaving an iron-impoverished serpentine.

A major chemical variation in the weathered lizardites is the negative correlation of Mg with Ni and Fe. Figure 2 shows that nickel increases more rapidly than iron but is correlated with it. The Fe level in unweathered serpentine, 0.1 to 0.2 atoms *per* 14 oxygens, is far higher than the nickel level, <0.012 atoms *per* 14 oxygens (Table 1). In the most substituted specimens the iron level has increased to over 0.3 and the nickel has increased by at least an order of magnitude (Fig. 2, Tables 2, 3 & 4). This is in agreement with the general observation that in saprolites of nickeliferous laterite profiles, iron is concentrated residually, whereas nickel is imported by leaching from the upper lateritic levels of the profile and magnesium is strongly leached out of the profile (Trescases 1975, Golightly 1979a).

Generally, the Ni and Fe levels in the weathered lizardites (Tables 2, 3 & 4) are completely independent of the primary igneous mineral the lizardite replaced. This is in contrast to the levels in the unweathered pseudomorphs (Table 1). The Ni/Fe and Fe/Mg correlations (*r* ~0.6) are weaker than the Ni/Mg correlations (*r* ~0.85). This may reflect a variable, unknown amount of goethite inclusion in the probed areas. Alternatively, it may reflect a spatial inhomogeneity of the iron distribution inherited from the initial distribution of magnetite grains in the unweathered serpentine. The shift between the bulk analyses of the saprolite boulders between 9 and 12 m depth, and the microprobe analyses of textural units within the boulders (Fig. 3) indicate about 2.5% Fe present in a phase other than lizardite. This shift could represent about 5% goethite, which is qualitatively compatible with the amount of goethite seen in thin section. The larger shift between the bulk analyses of the saprolite boulders and the bulk analyses of the borehole samples and the mined bulk samples reflects the structure and chemical composition of gross saprolite zones, which consist of saprolite boulders in a more evolved, goethite-rich matrix.

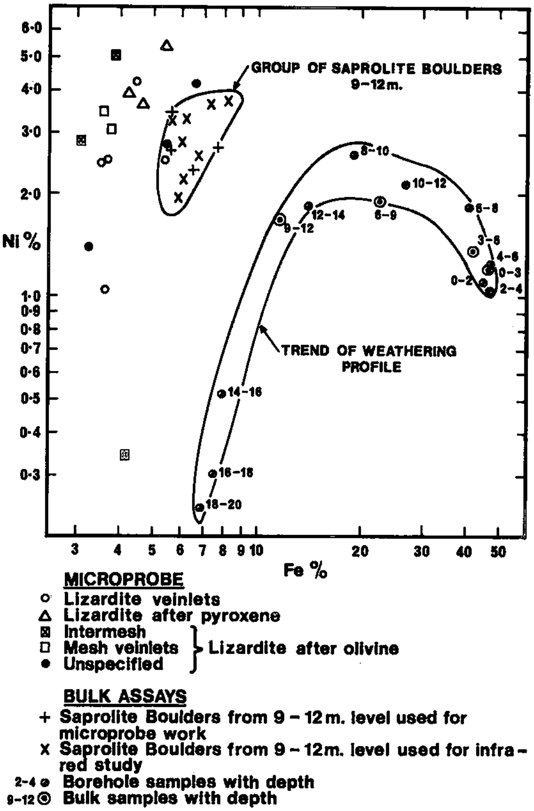

FIG. 3. Nickel and iron variation obtained by microprobe and in various bulk materials from the Soroako locality.

It is to be emphasized that the Ni/Fe correlation, both in microprobe and bulk analyses, is specific to the location and depends on the leaching history of the particular laterite profile. In this respect the present data differ from those of Brindley & Wan (1975), whose samples came from a worldwide variety of unrelated locations and showed no Ni/Fe correlation.

The microprobe data and the petrographic observations together suggest that a chemical reaction such as the following must be responsible for the initial disappearance of the magnetite micrograins and the initial increase in the Fe content of the serpentines:

$$9H_2O + \tfrac{1}{2}O_2 + \underset{\text{magnetite}}{2Fe_3O_4} + \underset{\text{serpentine}}{3Mg_3Si_2O_5(OH)_4}$$

$$\rightleftarrows \underset{\text{ferric serpentine}}{3Fe_2Si_2O_5(OH)_4} + 9Mg^{2+} + 18OH^-$$

Further decrease in Mg and increase in Ni could occur *via* the reactions:

$$\underset{\text{serpentine}}{Mg_3Si_2O_5(OH)_4} + 3Ni^{2+} \rightleftarrows \underset{\text{nickel serpentine}}{Ni_3Si_2O_5(OH)_4} + 3Mg^{2+}$$

$$\underset{\text{serpentine}}{Mg_3Si_2O_5(OH)_4} + 5H_2O \rightleftarrows 3Mg^{2+} + 2H_4SiO_4 + 6OH^-$$

The first of these proceeds strongly to the right (Golightly 1979a), whereas the second is the appropriate congruent dissolution reaction for serpentine (Hostetler & Christ 1968) in the alkaline environment (Trescases 1975, Golightly 1979a), at the base of nickeliferous laterite profiles in general. The joint action of these two reactions ensures (1) the enrichment of nickel leached from higher in the profile, (2) the net export of Si and Mg and (3) the residual concentration of iron generally observed in this class of nickeliferous laterites.

Aluminum and chromium

The second pattern evident in the data is the high Al_2O_3 and Cr_2O_3 levels in the bastite inherited from the pyroxene. Studies of laterite chemistry have generally shown Al, Fe and Cr to be relatively immobile in weathering compared to Si, Mg and Ca (Trescases 1975, Golightly 1979a). Specifically, in another location at Soroako, the concentration *per* unit volume of Al, Fe and Cr in saprolite was found to have decreased by 20%, 10% and nil, respectively, during the initial stages of saprolite formation (Golightly 1979b). At the same stage Mg, Ca and Si decreased by 85 to 95%. Thus the mutual ratios of Al, Fe and Cr should be relatively invariant during leaching, and assays renormalized to give Fe + Al + Cr = 100% should be useful for determining the relative changes in Fe, Al and Cr (Fig. 4).

In Figure 4, one can see through the progressive residual concentration of Fe, Al and Cr that occurs as a result of the selective leaching of Mg, Si and Ca described above. The cross and curved arrow on Figure 4 shows the actual variation of Al, Cr and Fe in the bulk material through the entire depth of the weathering profile and clearly indicate that these three elements remain in fixed proportion to each other. As shown below, this is far less than the changes that seem to have occurred in the minerals during serpentinization.

Whereas it can be argued that this procedure magnifies the error of measurement present in the low Al and Cr values, the scatter of data points in Figure 4 gives a clear measure of this error. Since the data are clustered in mineralogically distinct groupings, it is clear that statistically significant differences are visible in the figure.

The orthopyroxene pseudomorphs (Fig. 4) show the same Cr content but a strongly decreased Al content, compared to the orthopyroxenes themselves. However, there is no significant difference in Al or Cr contents of weathered and unweathered orthopyroxene pseudomorphs. Olivine pseudomorphs in both

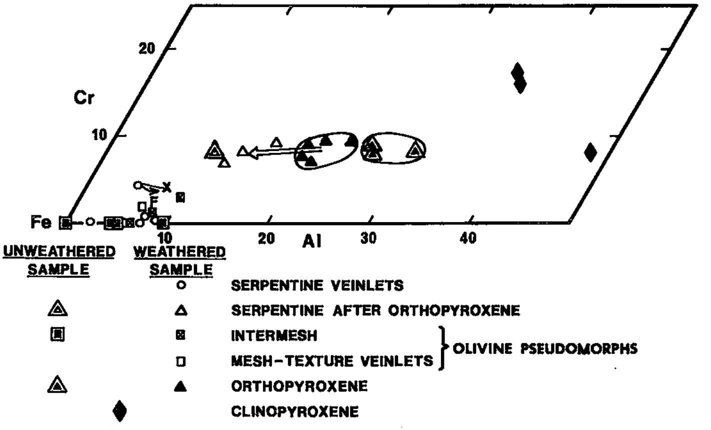

FIG. 4. Cr, Al and Fe levels in weathered and unweathered serpentines compared with those in orthopyroxene and clinopyroxenes from Soroako. The Cr, Al and Fe analyses have been renormalized to total 100% in order to overcome the obscuring effect of the general increase in Fe, Cr and Al that has occurred during lateritic weathering.

weathered and unweathered specimens show a significant increase in Al over olivine, which is virtually free of Al. Again there is no significant difference between weathered and unweathered olivine pseudomorphs. This pattern indicates a relative movement of Al and Fe, probably during serpentinization. Given the earlier conclusions about the iron–magnesium ratios in the unweathered lizardites, movement is best inferred as a movement of Al out of orthopyroxene pseudomorphs into olivine pseudomorphs during serpentinization.

Because of the amphoteric behavior of Al hydroxides, this centimetre-scale mobility of aluminum during serpentinization suggests that the solutions responsible for serpentinization are rather far from neutral pH. Since brucite is commonly present in serpentinites and since pH values in very dilute solutions in equilibrium with serpentine exceed 9 (Hostetler & Christ 1968), the serpentinization fluid is probably very alkaline.

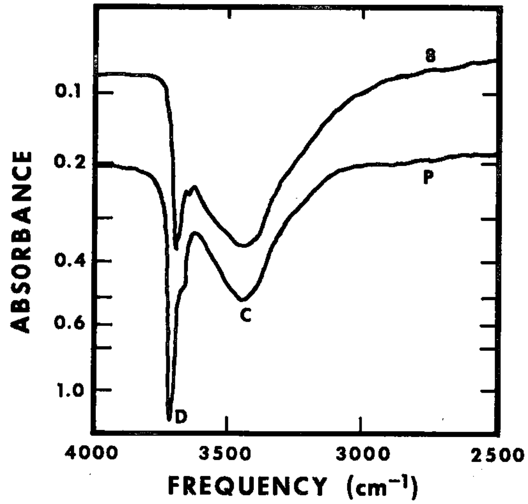

FIG. 5. The infrared spectrum of OH-stretching vibrations in pure (P) and nickel–iron substituted lizardite (#8. Table 5) from Soroako.

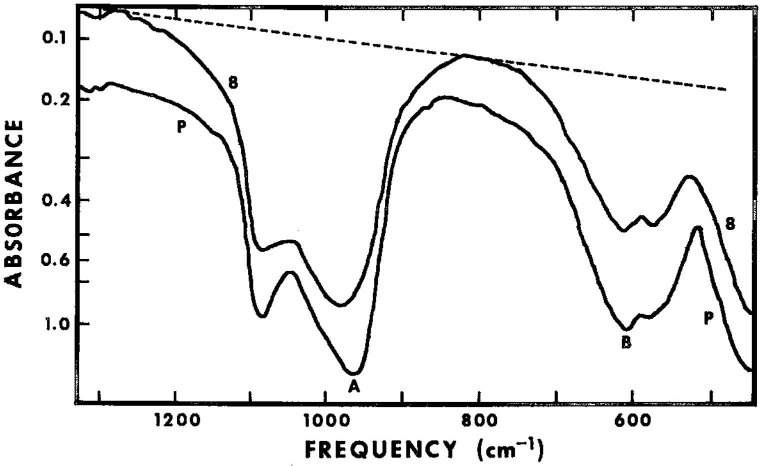

FIG. 6. The infrared spectrum of Si–O-stretching (A) and OH librational (B) vibrations in pure lizardite (P) and a nickel–iron substituted lizardite (#8, Table 5) from Soroako.

INFRARED-ABSORPTION SPECTRA

Infrared-absorption spectra were measured on eight samples from the same portion of the profile that provided the microprobe specimens. The spectra of three essentially pure lizardites, two from Thompson, Manitoba and one from the Canadian Refractories magnesite mine north of Calumet, Qué., were run for comparison. All have mesh textures and produce lizardite X-ray-diffraction patterns. The infrared spectrum of the metamorphic skarn lizardite from Calumet is very similar to the spectra of specimens from Soroako. The samples were prepared using 0.5 mg of material in the standard manner in KBr discs and were measured on a Perkin Elmer model 337 grating spectrophotometer.

The IR-absorption spectra of two samples of lizardite, one fresh and one strongly weathered, are shown in Figures 5 and 6. The ratio of the peak absorbance of the 610 cm^{-1} peak to that of the Si–O, 975 cm^{-1} peak is plotted in Figure 7 as a function of weight percent nickel. The ratio decreases as Ni substitution for Mg increases.

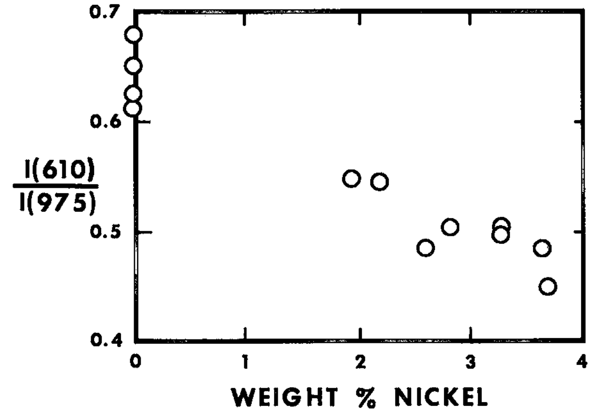

FIG. 7. The dependency of the infrared-absorption intensity ratio between Si–O stretching and OH librations on Ni substitution in lizardites from Soroako.

A nearly pure end-member nepouite from another locality at Soroako shows almost complete elimination of the peak at 610 cm^{-1}. The evidence thus clearly indicates that substitution of nickel for magnesium affects the 610 cm^{-1} band. This particular sample contains a certain amount of nickel kerolite (talc-like) impurity, however, so that the 663 cm^{-1} peak observed in synthetic nepouite (Stubican & Roy 1961) was obscured by the nickel kerolite spectrum. The reduction in intensity of the 610 cm^{-1} band, as shown in Table 5 and Figure 8, is directly proportional to the percentage of octahedral sites that have been substituted by Fe and Ni. There is a suggestion, indicated by the dashed line in Figure 8, that the dependence is quadratic, but this hypothesis is not a significant improvement over the linear relationship.

DISCUSSION OF INFRARED DATA

The infrared spectra of synthetic pecoraite and chrysotiles were reported by Stubican & Roy (1961). The study of various antigorites, chrysotiles and lizardites by Yariv & Heller-Kallai (1975) and the study of deuterium-substituted serpentines by Pampuch & Ptak (1970) have established the assignment of infrared absorption bands in lizardite as tabulated below (summarized from Yariv & Heller-Kallai 1975):

Frequency (cm^{-1})	*Assignment*
3700	OH stretching
1070–1085	Si–O stretching
1015–1025	
950–965	
630–650	Si–O bending ?
610–620	OH libration
560–585	Mg–O out of plane

According to Farmer (1974), numerous small peaks in the vicinity of 3700 cm^{-1} in phyllosilicates, in general, correspond to different combinations of cation neighbors in the adjacent octahedral sites. There is no gradual shift of OH stretching frequency with octahedral cation substitutions. Rather each peak, characteristic of each combination of neighbors, has an intensity proportional to the number of each of these combinations. This indicates that the OH vibrational wave function is highly localized rather than being a true lattice-vibration mode.

The 610–617 cm^{-1} peak in lizardite is rep-

TABLE 5. INTENSITY OF 610 AND 975 cm^{-1} ABSORBANCE BANDS IN NICKEL, IRON SUBSTITUTED SERPENTINES

	Weight Percent			Mole Percent	Observed		Calculated
Sample #	Nickel	Iron	Iron(Sp)	Magnesium Occupancy of Trioctahedral Sites x	I(610)/I(975) y	y/y^{100}	y/y^{100}
A	-	-	-	100	0.65	100.9	98.68
B	-	-	-	100	0.67	104.0	98.68
RR	-	-	-	100	0.61	94.7	98.68
P	-	-	-	100	0.625	97.0	98.68
1	1.94	5.9	4.35	88	0.548	85.0	86.45
2	2.20	6.05	4.70	86.3	0.547	84.9	84.0
3	2.6	6.68	5.3	84.5	0.485	75.3	81.3
4	2.8	6.00	5.5	83.7	0.506	78.6	80.0
5	3.29	5.80	5.9	82.0	0.500	77.6	77.2
6	3.29	6.18	5.9	82.0	0.507	78.7	77.2
7	3.65	7.33	6.2	80.5	0.486	75.5	74.5
8	3.70	8.09	6.2	80.2	0.452	70.2	74.0

The first three columns give assay data on the sample pulps. Iron(Sp) is the estimated solid solution iron calculated from the nickel assay and the Ni/Fe correlation known from microprobe data (assuming negligible iron in goethite). I(610)/I(975) is the intensity ratio of the 610 cm^{-1} Infrared Absorbance peaks, defined = y. y/y100 is the ratio in percent of this value to that in pure Mg-serpentine estimated as 0.644. y/y^{100} calculated is based on the quadratic regression formula.

$$y/y^{100} = -259.45 + 6.492\,X - 0.02911\,X^2$$

where X is the mole percent serpentine.

A and B are serpentines from Thompson, Man.; P from Calumet, P.Q.; and RR from Stubican & Roy (1961).

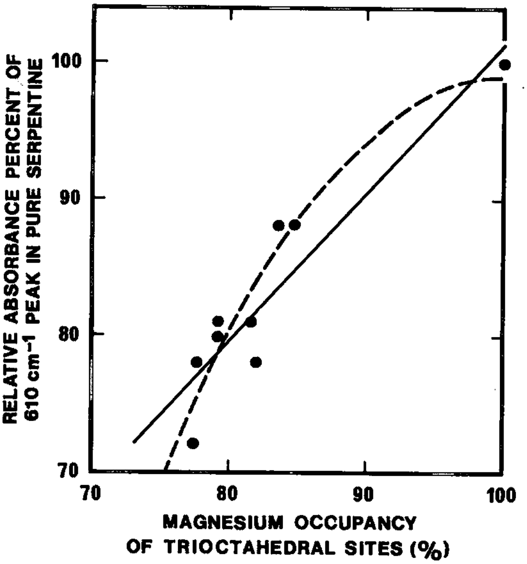

FIG. 8. The dependency of the infrared absorbance at 610 cm^{-1} in nickel–iron-substituted lizardites on the magnesium occupancy of trioctahedral sites. Solid line is a linear fit to the data, the dashed line a quadratic fit.

resented by a peak at 663 cm^{-1} in nepouite. A similar kind of frequency shift, 668 to 705 cm^{-1}, occurs in an OH librational band in talc and willemseite.

In the light of these data, the 610 cm^{-1} vibrational band in the present suite of samples must be an OH librational mode. The direct proportionality of the intensity of this band to the Mg occupancy of the octahedral layer suggests that, like OH stretching modes, the vibration is highly localized and reflects the proportion of OH bands with Mg ions in adjacent octahedral sites. There is no evidence in these samples, in which the amount of substitution is fairly limited, of new vibrational frequencies. However, the number of possible combinations is quite large. For example, such near-neighbor combinations would include: NiMgMg, NiNiMg, NiFeMg, FeFeMg and FeMgMg. Thus, a series of peaks of very low intensity, stretching out to the NiNiNi frequency of 663 cm^{-1} and an unknown frequency associated with Fe^{3+} substitution, should exist but may not be intense enough to be detected.

Whereas the direct proportionality of the intensity of the 610 cm^{-1} band to the Mg occupancy clearly supports the identification of this band as due to OH libration under the influence of nearby Mg ions, an exact proportionality with Mg occupancy is not expected. If the substitution of other ions or vacancies X for Mg were a homogeneous random distribution, the expected three-neighbor combinations would have the following probabilities (binomial distribution): XXX 0.8%, XXMg 10.6%, XMgMg 38.4% and MgMgMg 51.2%. Thus the unshifted (MgMgMg) OH libration should have 51.2% rather than ~80% of its intensity in Mg–lizardite as observed. The intensity could be closer to that observed if the OH librational wave functions were extensive lattice vibrations rather than localized modes, such as OH-stretching modes. If this were the case, however, the frequency would be shifted and the peak broadened, as is normal for lattice modes. The final alternative is that the substitution for Mg is a highly inhomogeneous one with a mosaic-like structure of relatively pure Mg and strongly substituted Ni and Fe^{3+} patches or zones.

Thus, a highly inhomogeneous and discontinuous substitutional mosaic, perhaps a layer-by-layer replacement, of Mg by Ni and Fe^{3+} is a possible explanation for the infrared absorption data. This mosaic would have to exist at a submicron scale, because the frequency distribution of the probe data does not indicate a marked mosaic pattern at the micron scale. It should be possible, though difficult, to confirm such a structure using advanced SEM, XRF or possibly high-energy TEM techniques.

CONCLUSIONS

The serpentinization process

Aluminum originally present in orthopyroxene is partially mobilized by the serpentinization reaction, whereas chromium is not. Thus, orthopyroxene pseudomorphs have a strongly reduced level of Al, whereas olivine pseudomorphs show a complementary increase in Al level. Nickel and chromium cations show less mobility.

The weathering process

Magnesium is leached away from, and iron is residually concentrated in serpentine. At the Soroako location, nickel is enriched at a much higher rate than is iron. The weathering process completely obliterates any distinctive difference in Ni and Fe contents between olivine- and pyroxene-derived lizardites. Weathering has no identifiable effect on the relative concentrations of Al, Fe and Cr at a micron scale.

The serpentine structure

Iron seems to be present as ferric iron, and the occupancy of the octahedral sites may be incomplete. The leached lizardite may be an intermediate structure between trioctahedral nickeliferous lizardite and a dioctahedral ferric equivalent of kaolinite.

The infrared-absorption spectrum

The 610 cm^{-1} absorbance peak is an OH libration mode specifically related to the presence of magnesium ions in adjacent octahedral sites. The rate of intensity decrease with cationic substitution suggests that Ni, Fe substitution for Mg is very inhomogeneous on a submicroscopic scale.

REFERENCES

ARANCIBIA, O.N. (1975): *Mineralogy and Chemistry of Two Nickeliferous Laterite Soil Profiles, Soroako Sulawesi, Indonesia.* M.Sc. thesis, Queen's Univ., Kingston, Ontario.

BRINDLEY, G.W. (1978): The structure and chemistry of hydrous nickel-containing silicate and aluminate minerals. *Bur. Rech. Géol. Minières Bull.* 2, 3, 233-245.

——— & WAN, H.M. (1975): Compositions, structures and thermal behavior of nickel-containing minerals in the lizardite–nepouite series. *Amer. Mineral.* **60**, 863-871.

ESSON, J. & CARLOS, L. (1978): The occurrence, mineralogy and chemistry of some garnierites from Brazil. *Bur. Rech. Géol. Minières Bull.* 2, 3, 263-274.

FARMER, V.C., ed. (1974): *The Infrared Spectra of Minerals.* Mineral. Soc., London.

GOLIGHTLY, J.P. (1979a): Nickeliferous laterites, a general description. *In* Proc. AIME Int. Laterite Symp. (D.J. Evans, R.S. Shoemaker & H. Veltman, eds.), 3-23.

——— 1979b): Geology of Soroako nickeliferous laterite deposits. *In* Proc. AIME Int. Laterite Symp. (D.J. Evans, & R.S. Shoemaker & H. Veltman, eds.), 38-56.

HOSTETLER, P.B. & CHRIST, C.L. (1968): Studies in the system $MgO–SiO_2–CO_2–H_2O$. I. The activity-product constant of chrysotile. *Geochim. Cosmochim. Acta.* **32**, 485-497.

LUCE, R.W. (1971): Identification of serpentine varieties by infrared absorption. *U.S. Geol. Surv. Prof. Pap.* **750-B**, 199-201.

PAGE, N.J (1967): Serpentinization at Burro Mountain, California. *Contr. Mineral. Petrology* **14**, 321-342.

PAMPUCH, R. & PTAK, W. (1970): Vibrational spectra and the structure of laminar silicates of 1:1 type. II. Octahedral layer. *Pol. Akad. Nauk, Oddzial Krakowie, Pr. Kom. Ceram., Ceram.* 14, 7-36 (in Pol.).

P.T. INTERNATIONAL NICKEL (1972): Laterite deposits in the south-east arm Sulawesi. *Nat. Inst. Geol. Mining Bandung* **4**, 37-57.

SOERIA-ATMADJA, R., GOLIGHTLY, J.P. & WAHJU, B.N. (1974): Mafic and ultramafic rock associations in the East Arc of Sulawesi. *Proc. Inst. Teknol. Bandung* 8, 67-85.

STUBICAN, V. & ROY, R. (1961): Isomorphous substitution and infra-red spectra of the layer lattice silicates. *Amer. Mineral.* **46**, 32-51.

TRESCASES, J.J. (1975): L'évolution géochimique des roches ultrabasiques en zone tropicale. *Mém. Orstom* 78.

WHITTAKER, E.J.W & ZUSSMAN, J. (1956): The characterisation of serpentine minerals by X-ray diffraction. *Mineral. Mag.* **31**, 107-126.

WICKS, F.J. & PLANT, A.G. (1979): Electron-microprobe and X-ray-microbeam studies of serpentine textures. *Can. Mineral.* **17**, 785-830.

——— & WHITTAKER, E.J.W. (1977): Serpentine textures and serpentinization. *Can. Mineral.* **15**, 459-488.

YARIV, S. & HELLER-KALLAI, L. (1975): The relationship between the IR spectra of serpentines and their structures. *Clays Clay Minerals* **23**, 145-152.

Received December 1978, revised manuscript accepted September 1979.